JOURNAL OF MATERIALS SCIENCE **35** (2000) 1069–1078

Fiber orientation and rheological properties of short fiber-reinforced plastics at higher shear rates

JIN KON KIM*, SANG HYUN PARK
Department of Chemical Engineering and Polymer Research Institute, Electric and Computer Engineering Division, Pohang University of Science and Technology, Pohang, Kyungbuk 790-784, Korea
E-mail: jkkim@postech.ac.kr

Fiber orientation and rheological properties of short fiber-reinforced polystyrene at high shear rates were investigated by scanning electron microscopy (SEM) and rheometry. This is the first attempt to observe fiber orientations in samples taken from inside the capillary as well as taken from the extrudate by employing SEM. The fiber orientations near the center of the capillary are similar to those near the wall. Also, the fiber orientations inside the capillary changed very little, even if the shear rate was varied from 25.4 to 3110 s^{-1}. This is because most fibers near the center as well as near the wall of the barrel are already aligned toward the flow direction before entering the capillary. The possible sources to induce surface roughness of the extrudate or fiber protrusion are discussed. It appears that the surface roughness depends mainly upon the velocity rearrangement at the capillary exit. Interestingly, fiber flexing was seen in the filament taken from the extrudate as well as from inside the capillary, which suggests that this is not likely a dominant source for inducing surface roughness.

1. Introduction

Short glass fiber-reinforced thermoplastics are composite materials used widely in industry since they have improved stiffness, mechanical strength, and heat distortion temperature compared with the base polymers. Owing to the anisotropic property of a composite, the maximum reinforcement can be obtained only when fibers are properly oriented [1]. The orientation of glass fibers in a composite is mainly influenced by flow characteristics during processing, and it significantly affects the rheological and mechanical properties of the composite.

Many research groups have reported that rheological properties such as viscosity and the first normal stress difference for glass fiber-reinforced polymers increase with increasing amount of glass fiber [2–13]. The fiber orientations and surface irregularities in the filament of the composite after an extrusion process were dependent upon shear rates and processing temperatures [7, 10, 14–17]. It was found that better surface smoothness of the filament of the composite is obtained with increasing shear rate.

Becraft and Metzner [10] investigated the rheological properties of glass fiber-filled polypropylenes using dynamic shear measurement and a capillary rheometer. They also studied fiber orientations and surface smoothness of the filament of the composite prepared by a capillary rheometer. The shear viscosity ($\eta(\dot{\gamma})$) of glass fiber-reinforced thermoplastics loading at lower shear rates, but the extent of increase in $\eta(\dot{\gamma})$ with increasing fiber content becomes smaller at higher shear rates. The surface roughness (or irregularities) of the filament of an extrudate was increased with decreasing shear rate, implying that these irregularities result from the complex flow related to fiber rotations and/or fiber flexing when the composite emerges from a capillary die.

Recently, we investigated the effect of the fiber orientation on the rheological properties of short glass fiber-reinforced plastics by using oscillatory shearing measurement [18]. When an oscillatory shearing is applied to the composites, the fiber orientations change and eventually reach steady values after longer times of oscillatory shearing. The rheological properties of the composite varied according to the change in fiber orientations; however, rather low shear frequencies and shear amplitudes were employed in the previous study. Thus, it is not easy to elucidate the effect of steady-shear rate on fiber orientations at very high shear rates, which have often been encountered in commercial applications such as injection and extrusion processes.

In this study, we investigated the rheological properties of short fiber-reinforced plastics at higher shear rates by using a capillary rheometer. It is the first attempt to observe fiber orientations in the filament of the composites taken from inside the capillary by using scanning electron microscopy (SEM).

* Author to whom all correspondence should be addressed.

2. Experimental

2.1. Material

The neat polymer employed in this study was a commercial grade of polystyrene (GPPS-G116; Dongbu Petrochemical Co., Korea). The weight average molecular weight (M_w) and the polydispersity index (M_w/M_n) are 322,000, and 2.3, respectively. The glass fiber employed in this study was a commercial product of Lucky-Dow Corning Co., Korea, with length of 3 mm and diameter of 13 μm. The preparation of glass fiber-reinforced PS with various amounts of glass fiber, hereafter referred to as filled PS, was described in a previous paper [18]. The average fiber length in filled PS was 0.7 ± 0.3 mm due to the breakage during the compounding.

2.2. Rheological measurement

A capillary rheometer (Instron Co., Model 4204) was used to measure shear viscosity (η) and shear stress

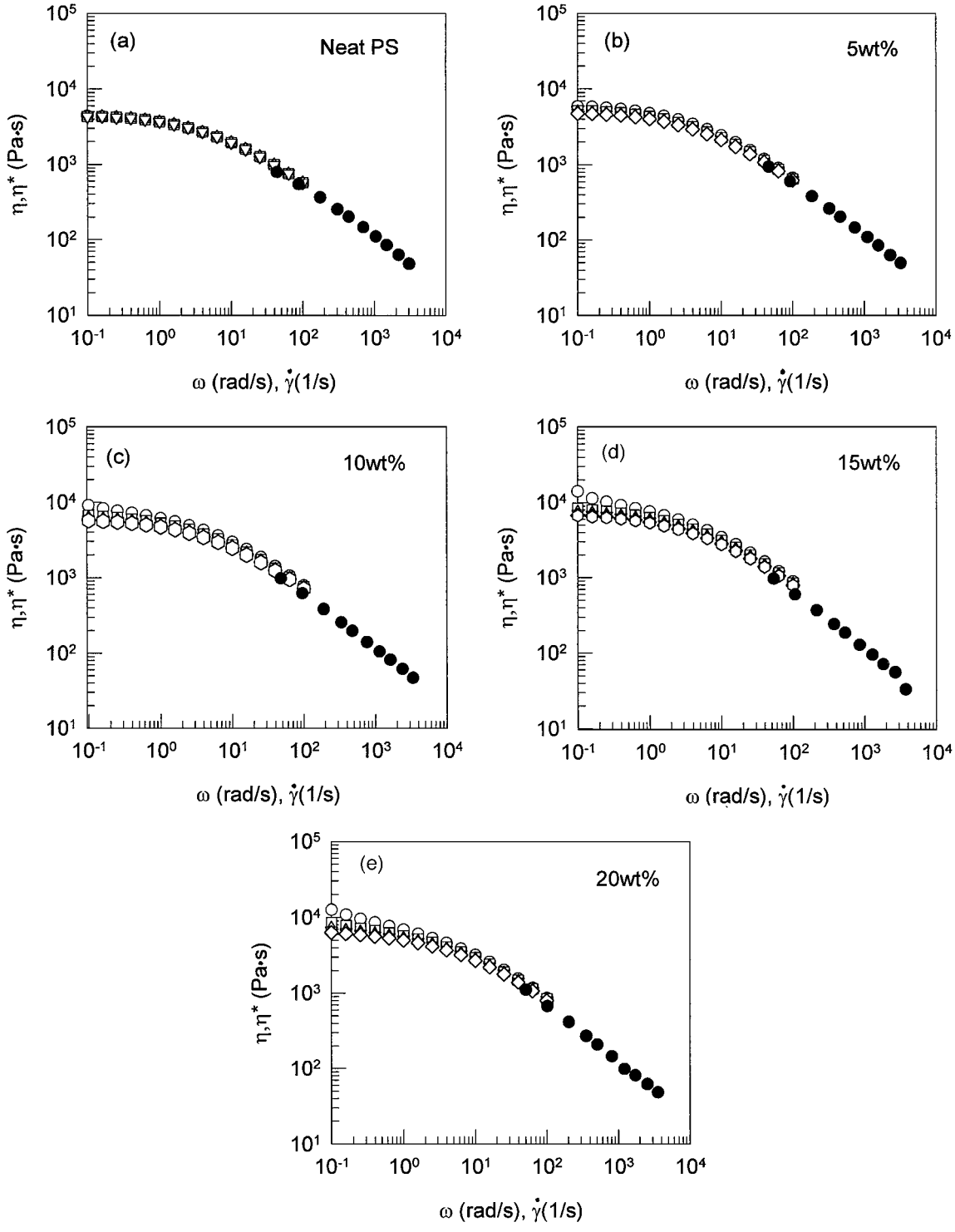

Figure 1 Plot of complex viscosity ($\eta^*(\omega)$) versus ω and plots of shear viscosity ($\eta(\dot{\gamma})$) versus $\dot{\gamma}$ at 220 °C for filled PS with various amounts of glass fibers (wt %): (a) 0 (neat PS); (b) 5; (c) 10; (d) 15; and (e) 20. Filled symbol (●) represents $\eta(\dot{\gamma})$ obtained from a capillary rheometer, and unfilled symbols represent $\eta^*(\omega)$ obtained from an oscillatory shearing measurement during the number of frequency sweep: (○) 1; (□) 2; (△) 3; (▽) 4; (◊) 5; and (⬭) 6.

at the wall (τ_w) as a function of the wall shear rate ($\dot{\gamma}_w$) of neat PS and filled PS at various temperatures. The length (L) and the diameter (D) of the capillary were 76.3 mm and 1.27 mm, respectively. Due to the very long capillary ($L/D = 60$), we did not use end-correction on Bagley plots to obtain the shear viscosity. However, the Rabinobitz correction was employed to obtain $\dot{\gamma}_w$. Also, an RDS-II (Rheometrics Inc.) using the dynamic oscillatory mode with parallel plates fixture (25 mm diameter) was used to measure complex viscosity ($\eta^*(\omega)$), the storage ($G'(\omega)$) and loss modulus ($G''(\omega)$) as functions of frequency (ω) of neat PS and filled PS at various temperatures. The strain amplitude was 0.15.

2.3. Morphological measurement

After measuring rheological properties of filled PS by the capillary rheometer at various shear rates and temperatures, we examined the fiber orientations in the filament of filled PS inside the capillary as well as in the extrudate by SEM. Because the capillary was quickly detached from the capillary rheometer after rheological measurement and put into an ice water mixture, it took ~50 s for filled PS in the molten state inside the capillary to reach a temperature lower than the glass transition of neat PS. Thus, it is considered that any change in fiber orientations of filled PS during the quenching was minimized. This suggests that the fiber orientations in a filament observed by SEM represent essentially the same as those inside the capillary. This is the first attempt to observe the fiber orientations of fiber-reinforced plastic inside the capillary by SEM. After cooling the capillary, we slowly removed the filament of filled PS in the capillary having a diameter of 1.27 mm from the capillary at room temperature by pushing a steel wire into the capillary. Finally, the filament was carefully cut into half, using a razor blade under liquid nitrogen environment, in the direction parallel to the axial direction of the filament (namely, the flow direction). An SEM image of longitudinal cross sections of the filament taken from the capillary as well as taken from an extrudate gives us better information of the variations in fiber orientations with the radial direction compared with an SEM image of sectors perpendicular to the filament. Then, the filament was coated with a thin layer of gold and the morphology was observed by a scanning electron microscope (Hitachi S 570).

3. Results and discussion

3.1. Rheological properties

Fig. 1 gives plots of complex viscosity ($\eta^*(\omega)$) versus ω (rad/s), and plots of shear viscosity ($\eta(\dot{\gamma})$) versus $\dot{\gamma}$ (1/s) at 220 °C for filled PS with various amounts of glass fibers. As reported in a previous paper [18], at lower frequencies (ω) $\eta^*(\omega)$ measured during the second frequency sweep is lower than that measured during the first frequency sweep, but this approaches a constant value as further frequency sweeps are made. This was attributed to the fact that initial random fiber orientations in filled PS prepared by compression molding were aligned steadily toward the flow direction during rheological measurements. It can be seen in Fig. 1 that when $\eta^*(\omega)$ is taken after many frequency sweeps, $\eta^*(\omega)$ is almost the same as $\eta(\dot{\gamma})$ for all fiber compositions employed in this study. Since the change in $\eta^*(\omega)$ with fiber contents at lower values of ω was already reported previously [18], in this study we focus on the viscosity change at higher shear rates measured by the capillary rheometer.

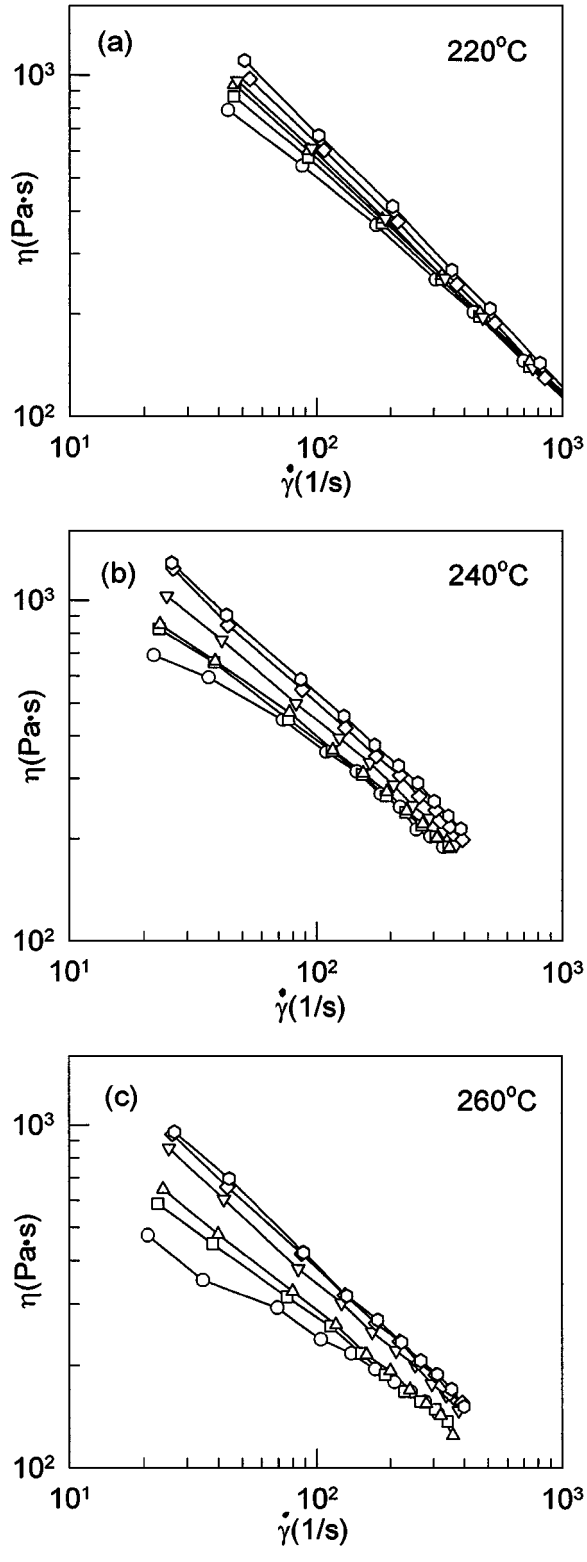

Figure 2 Plots of $\eta(\dot{\gamma})$ versus $\dot{\gamma}$ at three different temperatures for filled PS with various amounts of glass fibers (wt %): (○) 0 (neat PS); (□) 1; (△) 5; (▽) 10; (◇) 15; and (⬭) 20.

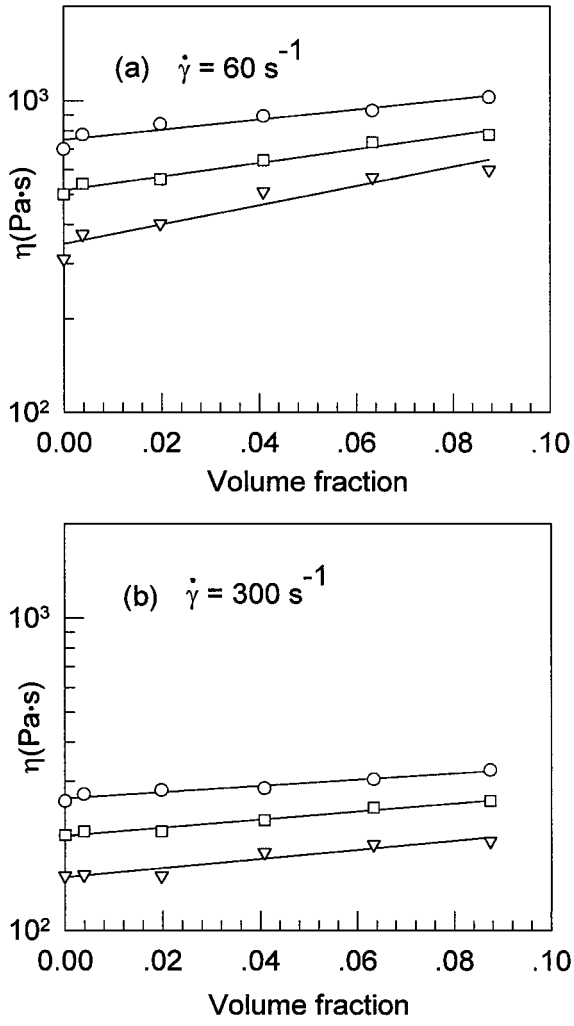

Figure 3 Plots of $\eta(\dot{\gamma})$ at two values of $\dot{\gamma}$ for filled PS versus volume fraction of glass fibers at three different temperatures; (○) 220 °C; (□) 240 °C; and (▽) 260 °C.

Plots of $\eta(\dot{\gamma})$ versus $\dot{\gamma}$ for filled PS with various fiber contents are given in Fig. 2a at 220 °C, in Fig. 2b at 240 °C, and in Fig. 2c at 260 °C, respectively. It can be seen in Fig. 2 that the increment in $\eta(\dot{\gamma})$ with fiber content is more evident with lowering $\dot{\gamma}$ and increasing measuring temperature. Plots of $\eta(\dot{\gamma})$ at $\dot{\gamma} = 60$ and 300 s^{-1} for filled PS versus volume fraction (c) of glass fiber as a function of measuring temperature are given in Fig. 3a and b, respectively. It can be seen that in the ranges of volume fractions employed in this study (i.e., c is less than 0.1) $\eta(\dot{\gamma})$ increases logarithmically with c. Previously we reported that the complex viscosity at lower frequencies increases logarithmically with c [18]. We also found that the values of the activation energy (ΔE) for filled PS decreases with increasing c and $\dot{\gamma}$. Notice that ΔE was obtained from the slope in plots of $\eta(\dot{\gamma})$ measured at constant $\dot{\gamma}$ versus the inverse of the temperature divided by the gas constant R. In two-phase systems, plots of $\eta(\dot{\gamma})$ versus shear stress (τ_w) are preferred to plots of $\eta(\dot{\gamma})$ versus $\dot{\gamma}$ since at the interface $\dot{\gamma}$ becomes discontinuous while τ_w is continuous [12]. Fig. 4 gives plots of $\eta(\dot{\gamma})$ versus τ_w at three different temperatures. It can be seen that the slope becomes steeper with decreasing temperature, and that shear viscosity does not vary much with glass fiber content at larger τ_w.

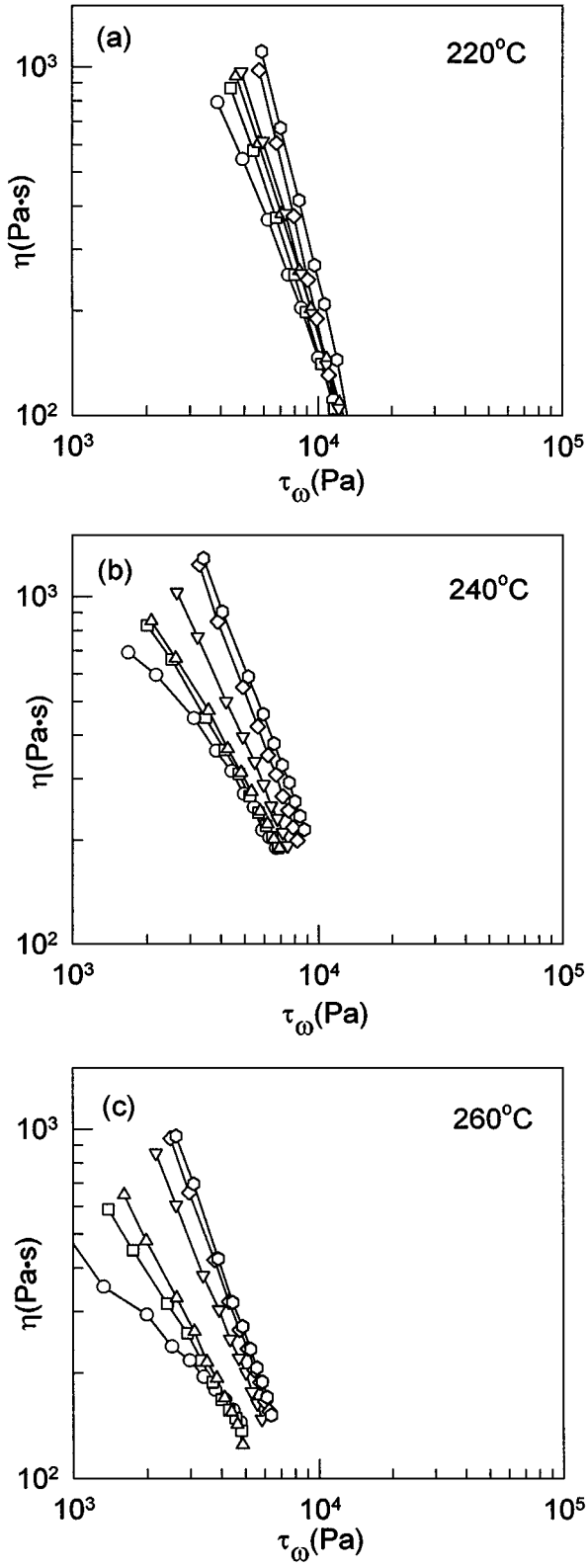

Figure 4 Plots of $\eta(\dot{\gamma})$ versus τ_w at three different temperatures for filled PS with various amounts of glass fibers (wt %). The symbols are the same as in Fig. 2.

3.2. Fiber orientations in filled PS

Fig. 5 gives fiber orientations in the cross section of a filament of filled PS with 10 wt % of glass fiber taken from near the exit of the capillary after measuring rheological properties at 240 °C and three different values of $\dot{\gamma}$, 25.4, 254, and 3110 s^{-1}. This is the first attempt to see fiber orientations in short-fiber reinforced polymer materials inside the capillary rheometer by SEM.

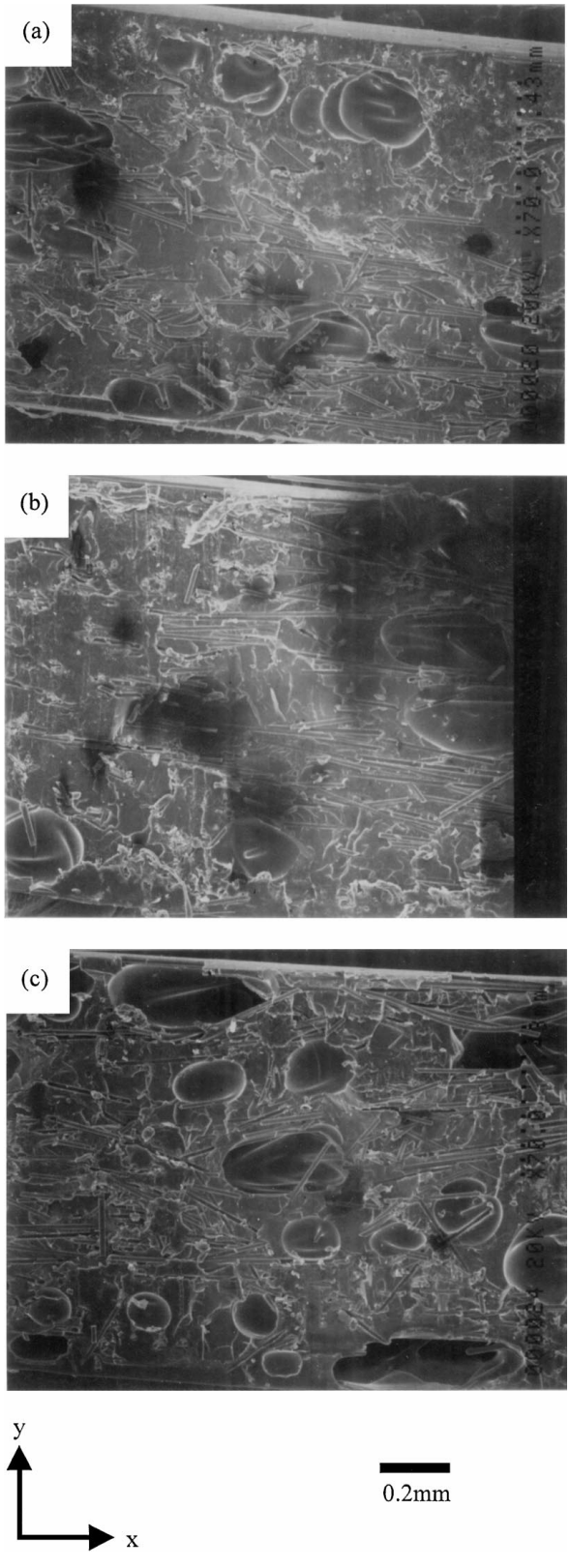

Figure 5 Fiber orientations in the cross-section of a filament of filled PS with 10 wt % of glass fiber taken from near the exit of the capillary after measuring rheological properties at 240 °C and three different values of $\dot{\gamma}$ (s^{-1}): (a) 25.4; (b) 254; and (c) 3110. Here, x-axis is the flow direction, and y-axis is the radial direction covering the diameter entire of the filament (from wall to wall).

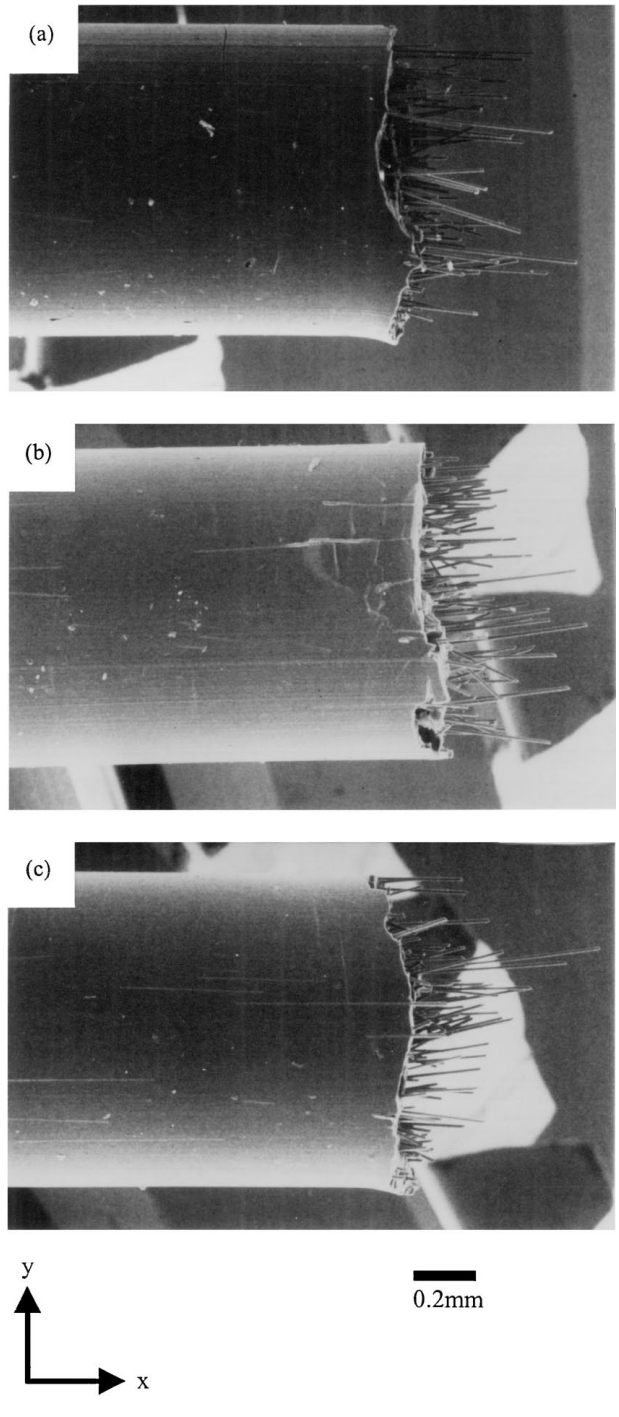

Figure 6 Fiber orientations in the filament of filled PS with 10 wt % of glass fiber taken from near the exit of the capillary after rheological properties were measured at 240 °C and three different values of $\dot{\gamma}$ (s^{-1}): (a) 25.4; (b) 254; and (c) 3110.

When the filament was cracked under liquid nitrogen environment, the fiber orientations in the filament were also qualitatively determined, as shown in Fig. 6. Notice that due to a rather poor adhesion between the matrix (PS) and fibers, the PS was easily detached from the fibers during the cracking. Thus, there remained fibers protruding normal to the fracture surface. It was unexpected to find from Figs 5 and 6 that most fibers were aligned toward the flow direction. And the fiber orientations inside the capillary changed very little, if at all, even when the shear rate varied greatly from 25.4 to 3110 s^{-1}. It should be mentioned that due to rapid quenching of the capillary described in the experimental section, the fiber orientations given in Figs 5 and 6 are essentially the same as those during rheological measurement under the specific shear rate. Fig. 7 gives SEM images taken at three axial positions, near the entrance, the middle, and near the exit, of the capillary

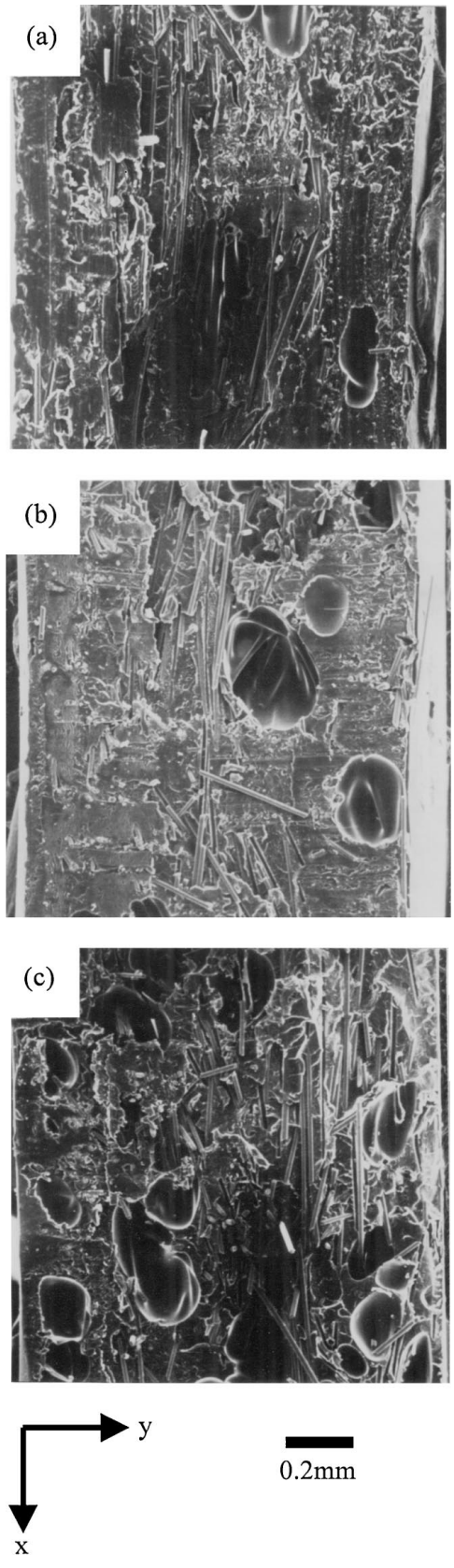

Figure 7 Fiber orientations in the cross-section of a filament of filled PS with 10 wt % of glass fiber taken from three different positions of the capillary after rheological properties were measured at 240 °C and $\dot{\gamma} = 25.4\ s^{-1}$. (a) near the entrance; (b) the middle; and (c) near the exit of the capillary.

for filled PS with 10% of glass fibers after measuring at 240 °C and 25.4 s^{-1}. Here, the x-axis is the flow direction, and the y-axis is the radial direction covering the entire diameter of the filament. One can note from

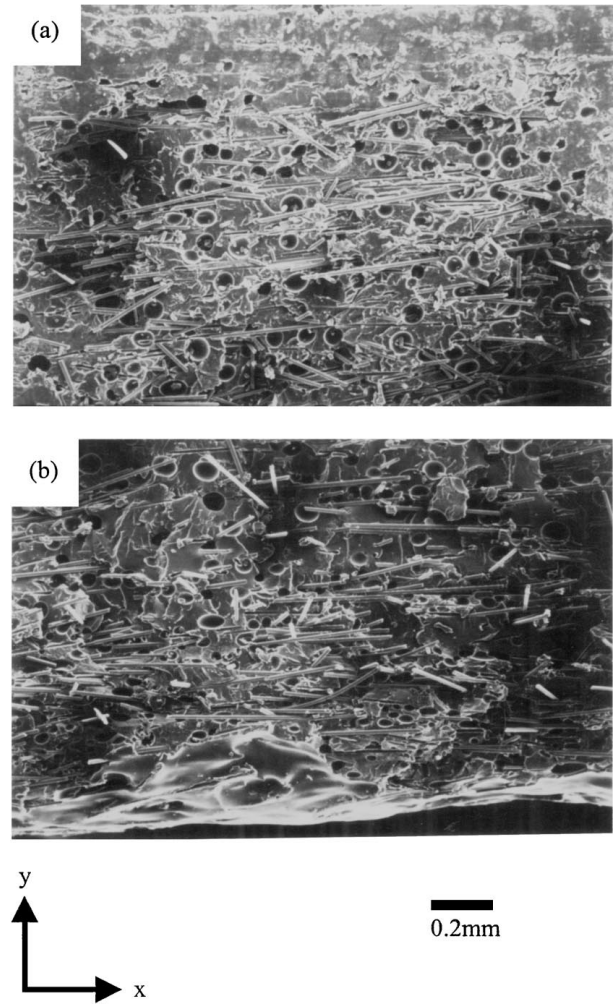

Figure 8 Fiber orientations in the cross-section of a filament of filled PS with 10 wt % of glass fiber taken from near the exit of the barrel after rheological properties were measured at 240 °C and $\dot{\gamma} = 25.4\ s^{-1}$. (a) near the center; (b) near the wall of the barrel.

Fig. 7 that fiber orientations do not change with axial direction of the capillary.

The absence of significant change in fiber orientation with radial position as well as with the shear rate is attributed to the fact that most fibers located near the center as well as near the wall of the capillary are already aligned toward the flow direction before entering the capillary. This is clearly demonstrated in Fig. 8 where most fibers inside the barrel of the rheometer are aligned toward the flow direction regardless of radial positions of the barrel. This behavior was previously reported by Crowson *et al.* [15] who employed an X-ray technique to investigate fiber orientations. It should be mentioned that the barrel diameter (9.525 mm) is much larger than the average fiber length (0.7 mm). We also found that most fibers in the filled PS with small content (e.g. 1 wt %) of glass fiber were aligned toward the flow direction regardless of radial positions of the barrel. This suggests that fiber-fiber interaction cannot be neglected even for filled PS with small amounts (say, 1 wt %) of glass fiber. Therefore, we conclude that the change in fiber orientation with the radial direction inside the capillary becomes very small.

Fig. 9 gives fiber orientations in the filament of the filled PS with 10 wt % of glass fiber taken from the

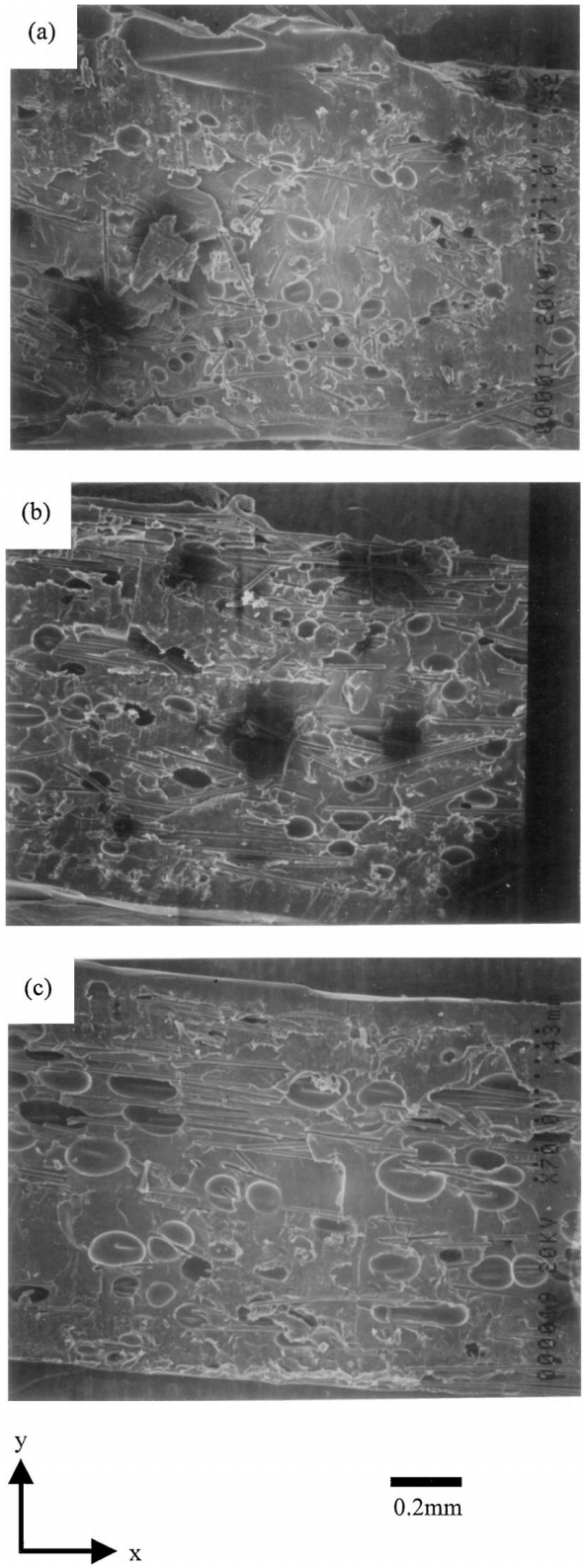

Figure 9 Fiber orientations in the cross-section of a filament of filled PS with 10 wt % of glass fiber taken from the extrudate after rheological properties were measured at 240 °C and three different values of $\dot{\gamma}$ (s^{-1}): (a) 25.4; (b) 254; and (c) 3110.

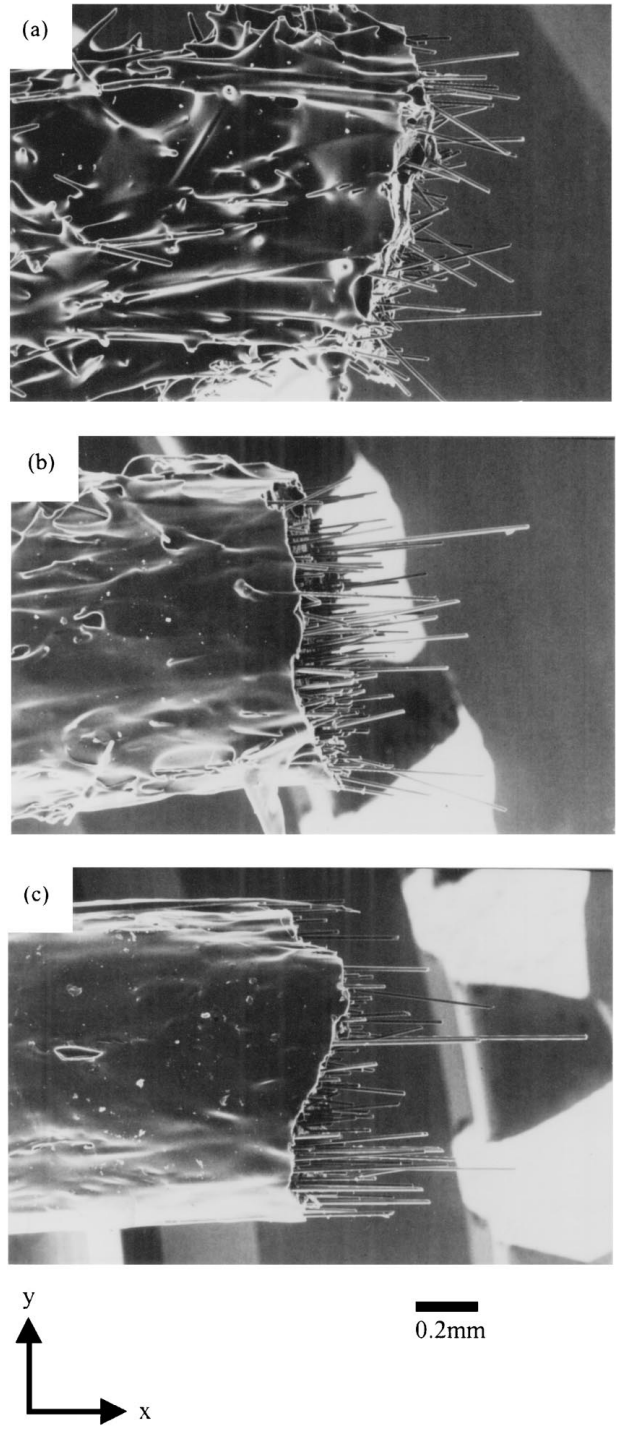

Figure 10 Fiber orientations in the filament of filled PS with 10 wt % of glass fiber taken from the extrudate after rheological properties were measured at 240 °C and three different values of $\dot{\gamma}$ (s^{-1}): (a) 25.4; (b) 254; and (c) 3110.

extrudate after the rheological properties were measured at 240 °C and three different values of $\dot{\gamma}$, 25.4, 254, and 3110 s^{-1}. At the $\dot{\gamma} = 25.4$ s^{-1}, many fibers protrude from the surface of the extrudate; thus the surface of the filament becomes rough. As the shear rate increases, the extrudate surface becomes smoother. This behavior was more evident when the extrudate was cracked, as shown in Fig. 10, or when optical micrograph (OM) images were taken from the extrudates as shown in Fig. 11. These results are consistent with previous reports [10, 14–16]. It can be further noticed that in the filament experiencing lower shear rates, a few fibers have more and less random orientations compared with the filament taken from inside the capillary, although most fibers are oriented toward the flow directions.

The surface roughness of the extrudate or fiber protrusion is due either to the velocity rearrangement at the capillary exit or to the fiber flexing. According to

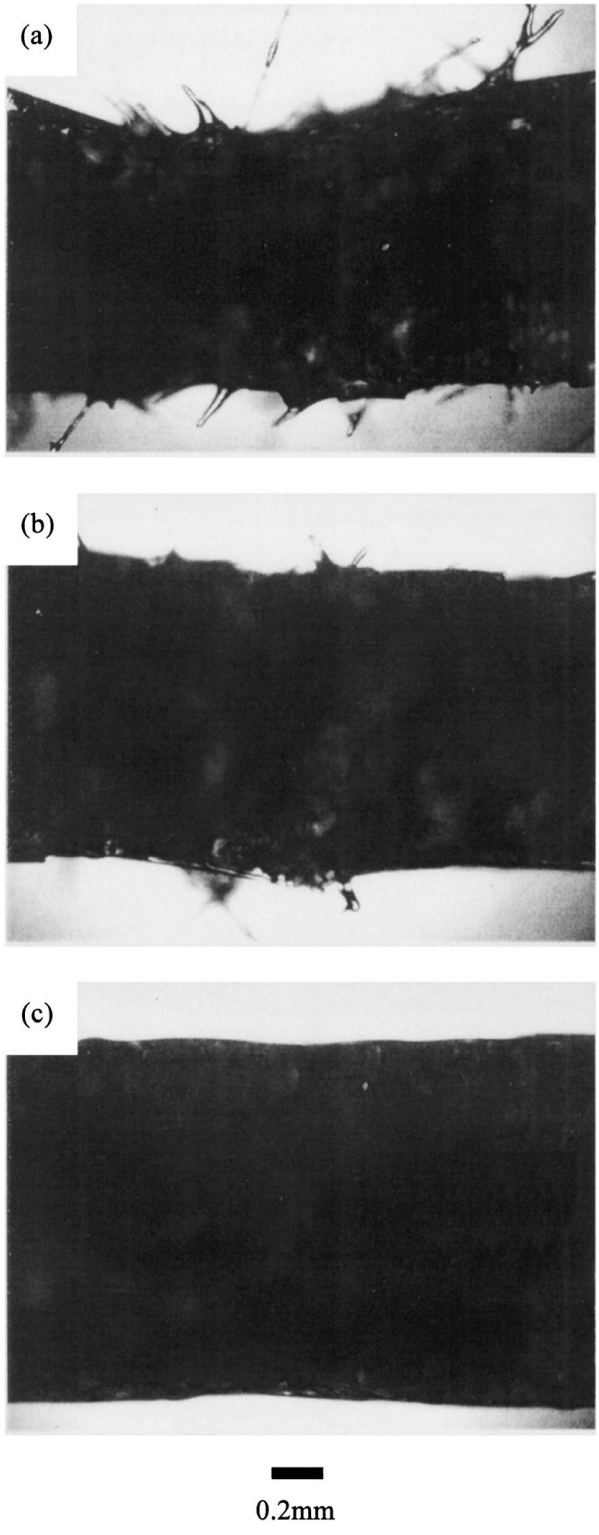

Figure 11 Optical micrograph (OM) images of the extrudates of filled PS with 10 wt % of glass fiber after rheological properties were measured at 240 °C and three different values of $\dot{\gamma}$ (s^{-1}): (a) 25.4; (b) 254; and (c) 3110.

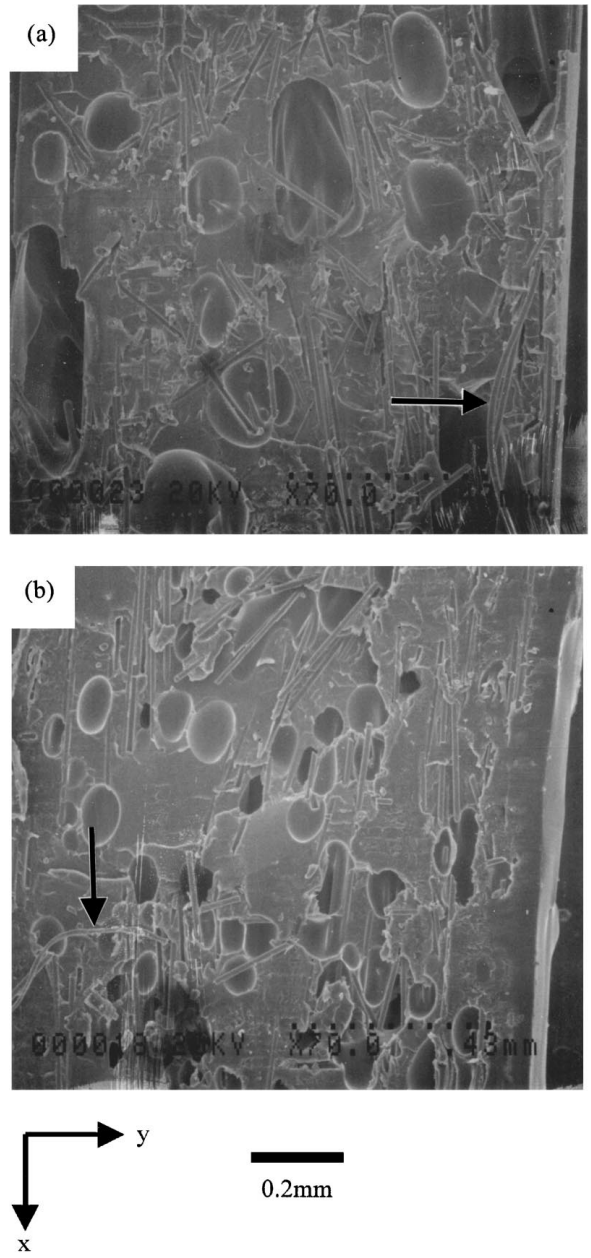

Figure 12 SEM images showing fiber flexing (marked by the arrow) in the filament of filled PS with 10 wt % of glass fiber after rheological properties were measured at 240 °C and $\dot{\gamma} = 3110\ s^{-1}$: (a) taken from inside the capillary and (b) taken from the extrudate.

numerical results given by Becraft and Metzner [10], the orientations of fibers near the wall are changed significantly compared with those near the center. It is noted that the velocity profile of the extrudate becomes the same regardless of the radial positions at the capillary exit, while the velocity of the molten sample inside the capillary is largest at the center. Thus, the velocity difference between the extrudate and molten composite inside the capillary near the exit is the largest at the wall. To compensate for the velocity difference, the fibers that are already aligned toward the flow direction inside the capillary can be rearranged in the extrudate to have orientations that deviate from the flow direction. However, at higher shear rates, the time for fibers in the extrudate to be rearranged becomes shorter; thus a smoother surface of the extrudate is expected.

Interestingly, fiber flexing marked by the arrow was clearly seen at the filament taken from inside the capillary in Fig. 12a as well as in the extrudate in Fig. 12b; this phenomenon was more evident for long fiber. Although Becraft and Metzner [10] reported the existence of fiber flexing for the first time, Fig. 12 gives clear evidence. If perpendicular cross sections of the filament were observed using SEM, one could not detect the existence of fiber flexing. However, although fiber flexing may affect fiber protrusion from the surface, it is not

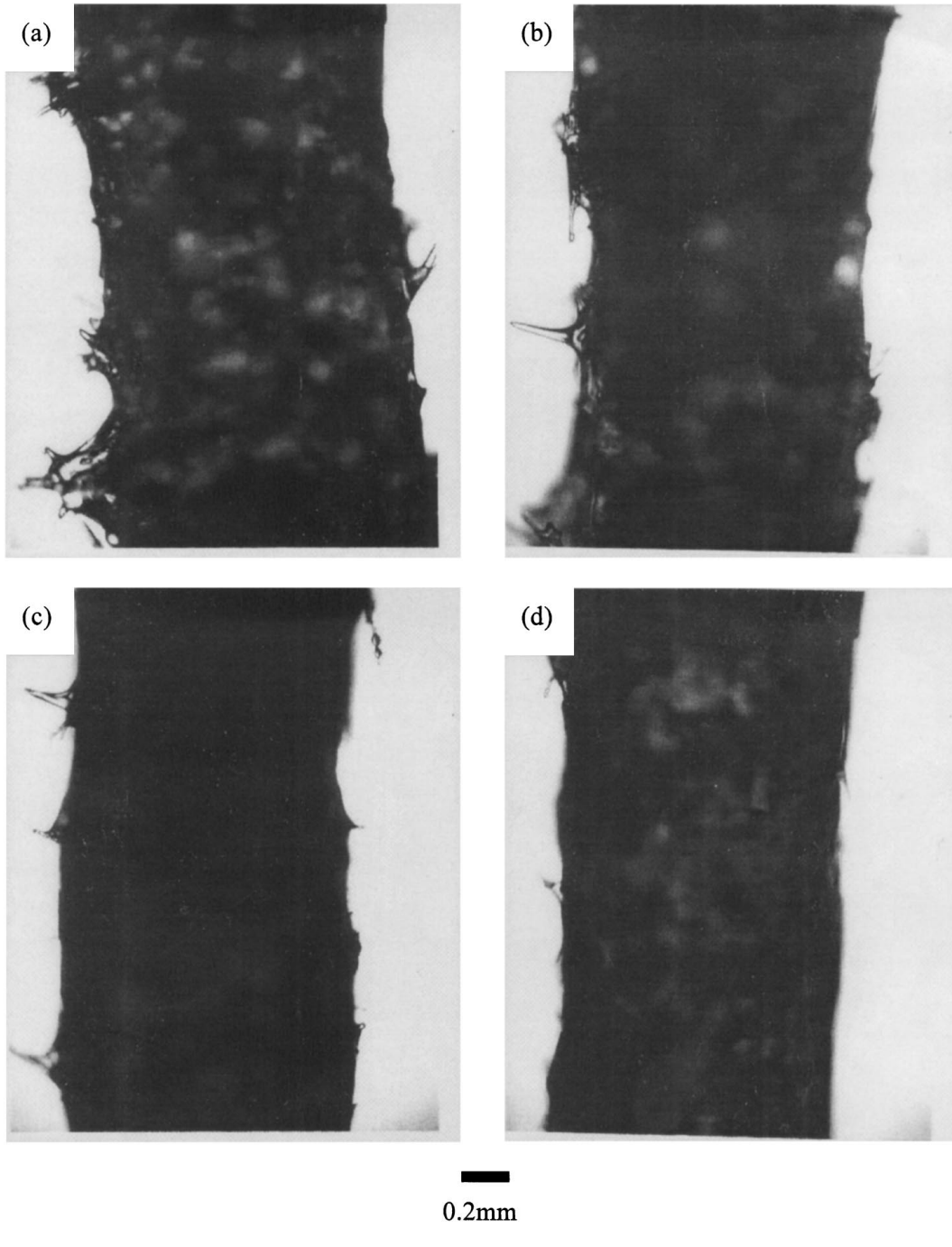

Figure 13 OM images of the extrudates of filled PS with 10 wt % of glass fiber after rheological properties were measured at different temperatures and shear rates: (a) 260 °C and 81.3 s^{-1} (τ_w = 3130 Pa); (b) 260 °C and 203.3 s^{-1} (τ_w = 4500 Pa); (c) 220 °C and 76.4 s^{-1}; (τ_w = 4600 Pa); (d) 220 °C and 191.0 s^{-1} (τ_w = 6890 Pa).

likely a dominant source of surface roughness. This is because fiber flexing was also seen in the extrudate (see Fig. 12b) when processed at much higher shear rates (e.g., 3130 s^{-1}). We also found the existence of fiber flexing in the extrudate as well as in the capillary at lower shear rate (e.g., 25.4 s^{-1}).

Based on the results given in Figs 10 and 11, one can speculate that the surface smoothness of the extrudate depends mainly upon the shear rate. However, because we consider that the surface smoothness or fiber protrusion is mainly due to velocity rearrangement near the exit of the capillary, the relaxation time of a filled polymer plays an important role in addition to shear rate. Therefore, the surface smoothness seems to be dependent upon the shear stress (τ). In other words, the extrudates after experiencing similar shear stresses exhibited similar surface roughness. Also, the larger the τ, the smoother the surface that is expected. This implies that with decreasing measuring temperature and increasing shear rate, the extrudate surface is expected to be smoother. Fig. 13 gives the surface roughness of the extrudates experienced at different temperatures and shear rates. It can be seen from Fig. 13b and c that even for large difference in temperature and shear rate (260 °C and 203.3 s^{-1} to 220 °C and 76.4 s^{-1}), the surface smoothness of the extrudate becomes similar for the two cases. Notice that the stress values for the two cases are very similar (4500 Pa versus 4600 Pa).

We also found that when an orifice ($L/D = 0$) was employed, the surface of the extrudate became very smooth even at lower shear rates and high temperatures (for instance, 25.4 s^{-1} and 260 °C), which is consistent with the result reported by Becraft and Metzner [10]. This is attributed to the fact that in this case no velocity rearrangement is expected. These results suggest that the surface roughness is mainly due to the velocity rearrangement of the fibers located at the wall at the capillary exit. The above argument is also consistent with the results by Wagner *et al*. [17] who reported that the fiber orientations in the extrudate become more random with increasing quenching time for the extrudate, namely slow cooling the filament from molten state. The results given in Figs 5–13 will help to develop a theory that enables one to predict the fiber orientations of the extrudate after a die swelling.

4. Concluding remarks

In this study, we have shown that for filled polystyrene with weight fraction of fiber less than 0.20, $\eta^*(\omega)$ is almost the same as $\eta(\dot{\gamma})$ when η^* is taken after many frequency sweeps. An increase in η with fiber content was evident on increasing measuring temperature and decreasing shear rate.

It is the first attempt to observe fiber orientations in the filament of the composites taken from inside the capillary by employing SEM. We found that the fiber orientations near the capillary center were similar to those near the capillary wall, and the fiber orientations inside the capillary changed very little even when the shear rate was greatly varied from 25.4 to 3110 s^{-1}. This is due to the fact that most fibers located near the center as well as near the wall of the barrel are already aligned toward the flow direction before entering the capillary.

It was considered that surface roughness of the extrudate or fiber protrusion is mainly due to the velocity rearrangement at the capillary exit; thus it depends upon the shear stress (τ). The larger the τ, the smoother the surface of the extrudate is expected to be. This implies that with decreasing measuring temperature and increasing shear rate, the extrudate surface becomes smoother. Although we clearly demonstrate the existence of fiber flexing in the filament taken from inside the capillary, this is not likely a dominant source affecting surface roughness, because fiber flexing was also observed in the extrudate.

Acknowledgement

This work was supported by Korea Research Foundation (1998), Korea.

References

1. C. L. TUCKER III and S. G. ADVANI, in "Flow and Rheology in Polymer Composites Manufacturing," edited by S. G. Advani (Elsevier, New York, 1994).
2. Y. CHAN, J. L. WHITE and Y. OYANAGI, *J. Rheol.* **22** (1978) 507.
3. V. M. LOBE and J. L. WHITE, *Polym. Eng. Sci.* **19** (1979) 617.
4. H. TANAKA and J. L. WHITE, *ibid*. **20** (1980) 949.
5. L. CZARNECKI and J. L. WHITE, *J. Apply. Polym. Sci.* **25** (1980) 1217.
6. B. CHUNG and C. COHEN, *Polym. Eng. Sci.* **25** (1985) 1001.
7. H. M. LAUN, *Coll. Polym. Sci.* **262** (1984) 257.
8. A. VAXAM, M. NARKIS, A. SIEGMANN and S. KENIG, *Polym. Compos*. **10** (1989) 78.
9. G. AUSIAS, J. F. AGASSANT, M. VINCENT, P. G. LAFLEUR, P. A. LAVOIE and P. J. CARREAU, *J. Rheol.* **36** (1992) 525.
10. M. L. BECRAFT and A. B. METZNER, *ibid*. **36** (1992) 143.
11. J. P. GREENE and J. O. WILKES, *Polym. Eng. Sci*. **35** (1995) 1670.
12. C. D. HAN, "Multiphase Flow in Polymer Processing" (Academic Press, New York, 1981).
13. J. L. WHITE, "Principles of Polymer Engineering Rheology" (John Wiley & Sons, New York, 1990).
14. S. WU, *Polym. Eng. Sci.* **19** (1978) 638.
15. R. J. CROWSON, M. J. FOLKES and P. F. BRIGHT, *ibid.* **20** (1980) 925.
16. B. A. KNUTTON and J. L. WHITE, *J. Appl. Polym. Sci.* **26** (1981) 2347.
17. A. WAGNER, R. YAZICI and D. M. KALYON, *Polym. Compos.* **17** (1994) 840.
18. J. K. KIM and J. H. SONG, *J. Rheol.* **41** (1997) 1061.
19. W. P. COX and E. H. MERZ, *J. Polym. Sci.* **28** (1958) 619.
20. M. DOI and S. F. EDWARDS, "The Theory of Polymer Dynamics" (Clarendon Press, Oxford, 1986).

Received 21 June
and accepted 25 August 1999